Unprecedented early summer warming recorded in tree rings on the central eastern Tibetan Plateau over the past three centuries

Jiangfeng Shi[1,2] · Hui Wang[1] · Jinbao Li[3,4] · Shiyuan Shi[1] · Jiarui Xu[1] · Yaping Zhang[1] · Huayu Lu[1]

Abstract

The Tibetan Plateau is a fast-warming region in China, whereby the rapid temperature increase affects regional ecosystems and mountain glaciers significantly. Long-term high-quality temperature data are urgently needed to understand how temperature has changed in the past several centuries and the underlying driving forces. In this study, we developed two tree-ring width chronologies that are more than 300 years. The two chronologies are highly consistent, indicating that the two sites were seldom disturbed by human activities. A robust tree-ring width chronology was developed using all the samples of the two sites, which represents June-July mean temperature according to statistical correlation analysis. The recent two decades are the warmest over the past three centuries, showing a regional temperature response to global warming largely contributed by human influence on climate system. Multi-decadal temperature variations in the study area have been closely linked with the Atlantic Multidecadal Oscillation in the past three centuries, highlighting the Atlantic influence on regional climate change on the central eastern Tibetan Plateau in warm seasons.

1 Introduction

Global land-surface air temperature has risen rapidly since the late nineteenth century, and this warming has been particularly marked since the 1970s (Hartmann et al. 2013). The Tibetan Plateau (TP) is one of the most sensitive areas to global climate change (Liu and Chen 2000; Yao et al. 2019), and meanwhile it plays an important role in modulating large-scale atmospheric circulations and climate over Asia (Broccoli and Manabe 1992; Li and Yanai 1996; Wu et al. 2012). For example, the thermal conditions on the TP have a strong influence on the strength of the Asian summer monsoon that produces much of the urgently needed precipitation for the Asian continent (Fu et al. 2020; Xu et al. 2019). Although it is well acknowledged that the temperature increasing rate in the TP is higher than that in the Northern Hemisphere and the same latitudinal zone over the second half of the twentieth century (Liu and Chen 2000), its long-term variations, especially on decadal to multi-decadal scales, are still not well understood mainly due to two reasons. One is that the meteorological data are too short because most of the stations were built after 1958 (Wei et al. 2003). The other is that high quality temperature reconstructions based on paleoclimate proxy records are still limited for this extensive plateau.

Tree rings have characteristics of annual resolution and precise dating (Hughes 2002), and have been widely used for temperature reconstructions worldwide (Cook et al. 2000; Esper et al. 2002; Shi et al. 2017a). Many tree-ring based temperature reconstructions have been conducted in the southeastern TP (Bi et al. 2020; Bräuning and Mantwill 2004; Duan et al. 2019; Huang et al. 2019; Shao and Fan 1999; Shi et al. 2015, 2017b; Wang et al. 2015), and fewer in the northeastern TP (Gou et al. 2007, 2008; Liu et al. 2009). The southeastern TP is influenced by the Indian summer monsoon that brings a lot of moisture from the Indian

✉ Jiangfeng Shi
shijf@nju.edu.cn

[1] School of Geography and Ocean Science, Nanjing University, Nanjing 210023, China

[2] Collaborative Innovation Center of Climate Change, Nanjing 210023, China

[3] Department of Geography, University of Hong Kong, Pokfulam, Hong Kong SAR, China

[4] HKU Shenzhen Institute of Research and Innovation, Shenzhen 518057, China

ocean. It also features a low temperature due to high elevations. High precipitation and low temperature make trees growing there sensitive to temperature. On the other hand, the northeastern TP is located in inner continent with less precipitation, and as a result trees there are sensitive to precipitation other than temperature (Liu et al. 2006; Shao et al. 2010; Yang et al. 2021; Zhang et al. 2015). Understanding climate change on the eastern TP is complicated due to its large spatial extent and complex climate and orography. The transitional zone between the northeastern and southeastern TP, i.e., central eastern TP, is critical to understand the climate on the eastern TP. Previous studies suggest that tree growth in the central eastern TP is generally stressed by warm-season temperatures (Liang et al. 2008; Xiao et al. 2015; Zhu et al. 2016), which shows the potential for warm-season temperature reconstructions.

Our aims in this study are to (1) build a long, well-replicated tree-ring width chronology using the samples from two independent sites on the central eastern TP, (2) identify and reconstruct the most critical climate limiting factor on tree growth, (3) explore its spatial representativeness and validate its reliability by comparing with other nearby

temperature reconstructions, and (4) explore its major features and teleconnections with large-scale oceanic and atmospheric circulation modes.

2 Data and methods

2.1 Meteorological data

The study area is located in the eastern border of the TP, where the average elevation is higher than 3,000 m above sea level (a.s.l.). Influenced by alternations of the westerlies in winter and the Indian summer monsoon in summer, distinct dry and wet seasons can be found in this area. Meteorological data from three meteorological stations (Songpan, Hongyuan and Ruo'ergai) close to the sampling sites were used in this study (Fig. 1; Table 1). Climate parameters include monthly mean, maximum, and minimum temperatures, and monthly total precipitation. The common period of climate data from the three stations is from 1961 to 2015. Songpan station was relocated to a new site in 2013 that is a few kilometers away from the original one. Therefore, we
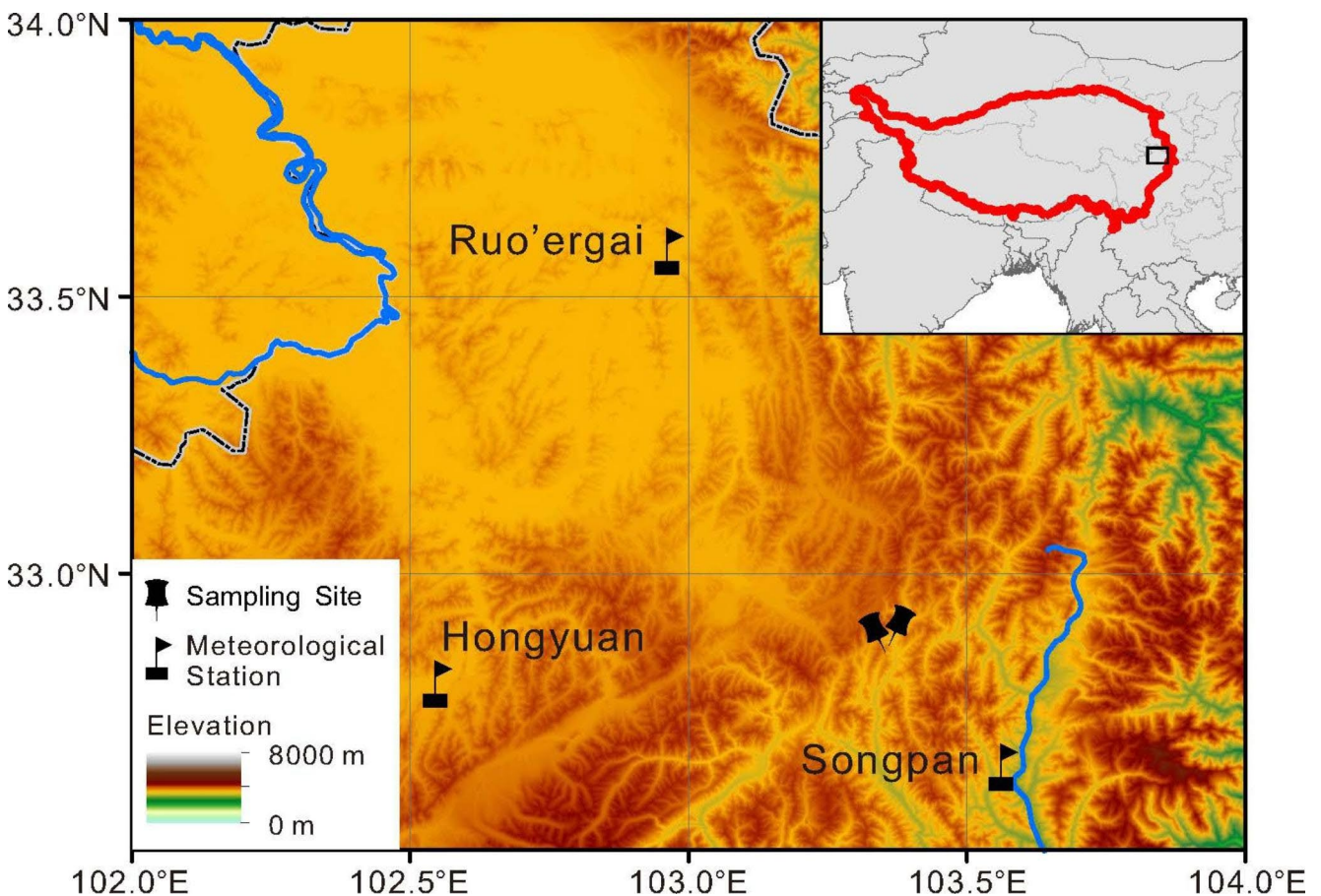
Fig. 1 Map showing the two tree-ring sampling sites and the three meteorological stations. The red line of the inset delineates the boundary of the TP

Table 1 Characteristics of the meteorological stations

Station	Latitude (N)	Longitude (E)	Altitude (m a.s.l.)	Time span (CE)	Annual mean temperature (°C)	Annual total precipitation (mm)
Songpan	32°39′	103°34′	2850.7	1951–2015	6.1	719
Hongyuan	32°48′	102°33′	3491.6	1961–2015	1.6	752
Ruo'ergai	33°35′	102°58′	3439.6	1957–2015	1.3	653
Region				1961–2015	3.0	708

adjusted Songpan temperature data from 2013 to 2015 by comparing the monthly differences between Songpan and the average of Ruo'ergai and Hongyuan over the periods 2013–2015 and 1961–2012. We did not adjust precipitation because it varies locally and is not the focus of this study. Meteorological data from the three stations were averaged to represent the regional situation (Fig. S1). The hottest month is July with a temperature of 12.3 °C, and the coldest is -7.8 °C in January. April-October is the rainy season, with a precipitation of 653 mm, accounting for 92.2% of the annual total precipitation.

2.2 Tree-ring data

Tree cores were collected from two sites, SP01 (32.87°N, 103.36°E, 3680 m a.s.l.) and SP02 (32.85°N, 103.36°E, 3650–3666 m a.s.l.). The two sites are 1.5 km away from each other in a straight distance. The dominant tree species is *Picea purpurea*, with a very small percentage of *Abies faxoniana*. Most of the trees from which we took cores are *P. purpurea*, with a few *A. faxoniana* trees collected as well. Only one core per tree was collected at SP01, and two cores per tree at SP02. All samples were mounted and sanded following standard procedures of Dendrochronology (Stokes and Smiley 1996). Each ring width was measured to a precision of 0.001 mm using a LINTAB 5.0 system after being visually cross-dated under a microscope. The quality of cross-dating was checked with the COFECHA program (Holmes 1983). Eventually, 53 cores from 53 trees at SP01 and 58 cores from 34 trees at SP02 were used in the following analyses.

The raw series of ring-width measurements were detrended using the program RCSigFree (http://www.ldeo.columbia.edu/tree-ring-laboratory/resources/software). Age-dependent spline was applied to detrend each raw series. Ring-width index was calculated as the ratio of actual ring-width and the estimated value, and the robust biweight mean was used to assemble the chronology (Cook 1985). The "signal-free" approach was applied to reduce potential trend distortion in tree-ring chronologies (Melvin and Briffa 2008). The mean inter-series correlation (Rbar) and the expressed population signal (EPS) were calculated for 51-year moving window (Wigley et al. 1984). The EPS threshold value of 0.85 was used to assess the most reliable period of the chronology.

2.3 Methods

Correlation and response functions (Fritts et al. 1970) were used to analyze the relationship between tree growth and climate. The response functions were calculated using the program DENDROCLIM2002 (Biondi and Waikul 2004). A linear regression function was applied to reconstruct June-July mean temperature, the main limiting factor on tree growth. A split sample calibration and verification method was used to assess the reliability of the reconstruction model. Spatial representativeness was explored using the KNMI (http://climexp.knmi.nl). Multi-taper method (MTM) spectral analysis (Mann and Lees 1996) was used to examine the frequency characteristics of the reconstruction.

3 Results

3.1 Characteristics of the tree-ring chronologies

Two site chronologies were built using the signal-free method (Fig. 2). The correlation coefficient between them is 0.75 over their common period 1701–2015, and 0.84 over their common reliable period 1748–2015 based on the EPS value higher than 0.85, both significant at 0.001 level. The correlation coefficient is 0.88 between their first differenced series over the period 1749–2015, significant at 0.001 level. Further considering that the straight distance between the two sites is only 1.5 km and that they have a similar elevation, we pooled all the samples from these two sites together to build a robust chronology, named SP0102 (Fig. 3). COFECHA results showed that for all raw measurements in SP0102, the mean segment length is 240 years, with a series intercorrelation of 0.62 and a mean average sensitivity of 0.14. The absent rings account for 0.04% of the total rings. The same method as used for site chronologies was used to develop the robust regional chronology, with a reliable period of 1730–2015 based on EPS higher than 0.85 (Fig. 3c). Only the robust chronology was used in the following analyses.

Fig. 2 a The tree-ring width chronology from SP01 (red) and SP02 (blue) sites. **b** Low-frequency ring width series with a 10-year fast Fourier transform (FFT) filter. **c** The sample size
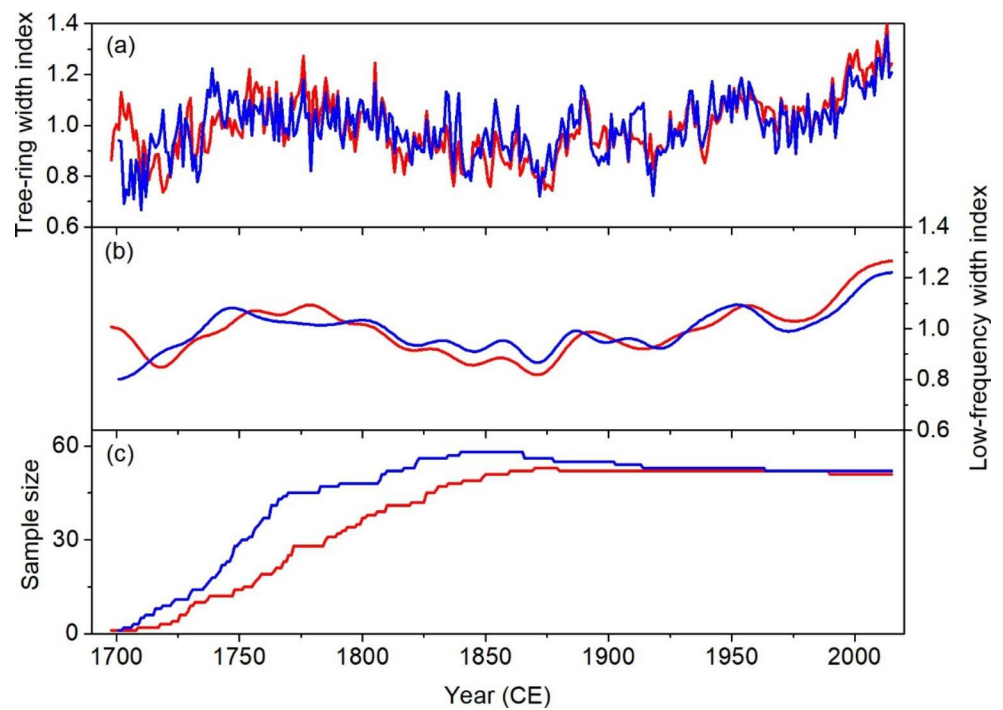
Fig. 3 a The tree-ring width chronology (thin black line) covering the past 318 years (AD 1698–2015) with a 10-year FFT filter (thick red line). **b** Rbar statistics calculated over 51-year window. **c** EPS statistics calculated over 51-year window. The dotted line denotes the 0.85 threshold value. **d** The sample size
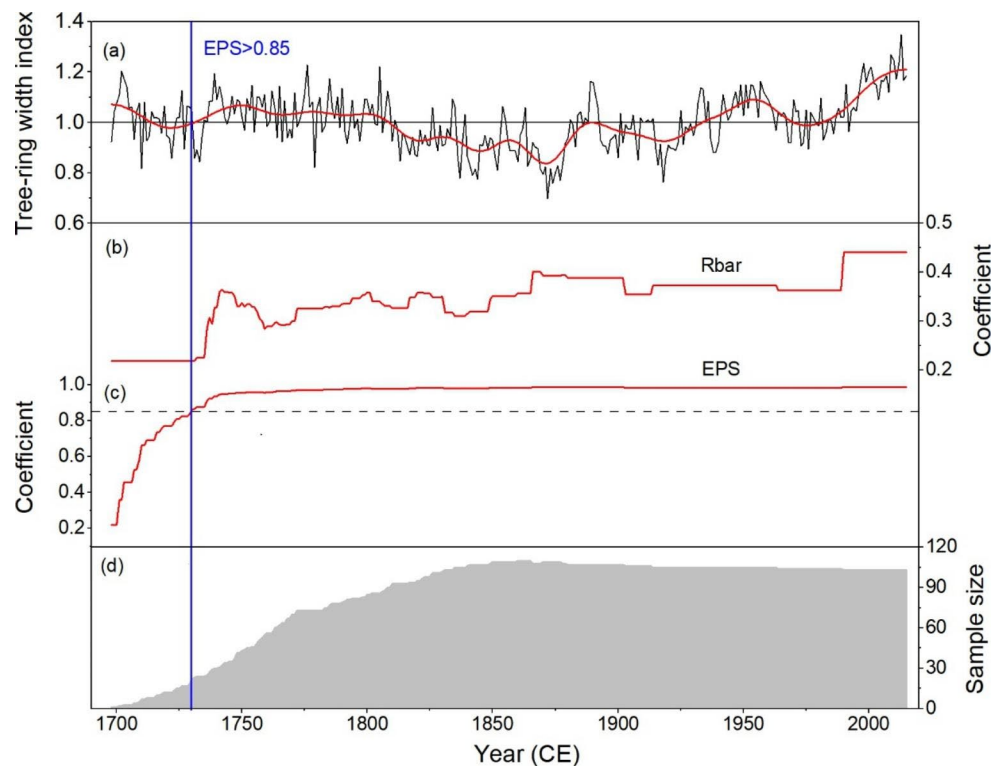
3.2 Relationships between tree growth and climate

Correlation analyses were conducted between the SP0102 chronology and monthly mean, maximum, minimum temperatures and monthly total precipitation in Songpan, Hongyuan, Ruo'ergai and the regional average from previous September to current October over the period 1961–2015. As shown in Fig. 4, there are quite similar patterns for Songpan, Ruo'ergai, Hongyuan, and their average. Therefore, we focus on the results of their average. Generally, tree growth correlates positively with monthly mean, maximum, and minimum temperatures. The correlations are the highest for

Fig. 4 Correlation coefficients (bar) and response functions (circle) between the chronology and **a** monthly mean temperature, **b** maximum temperature, **c** minimum temperature, and **d** precipitation based on Songpan, Hongyuan, Ruo'ergai meteorological data and the regional average over the period 1962–2015. The horizontal dashed lines denotes 99% confidence level for correlation coefficient. Response functions were only calculated for **a** regional monthly mean temperature and **d** monthly total precipitation. The black solid circle denotes significant value at 0.05 level. "p" means previous year
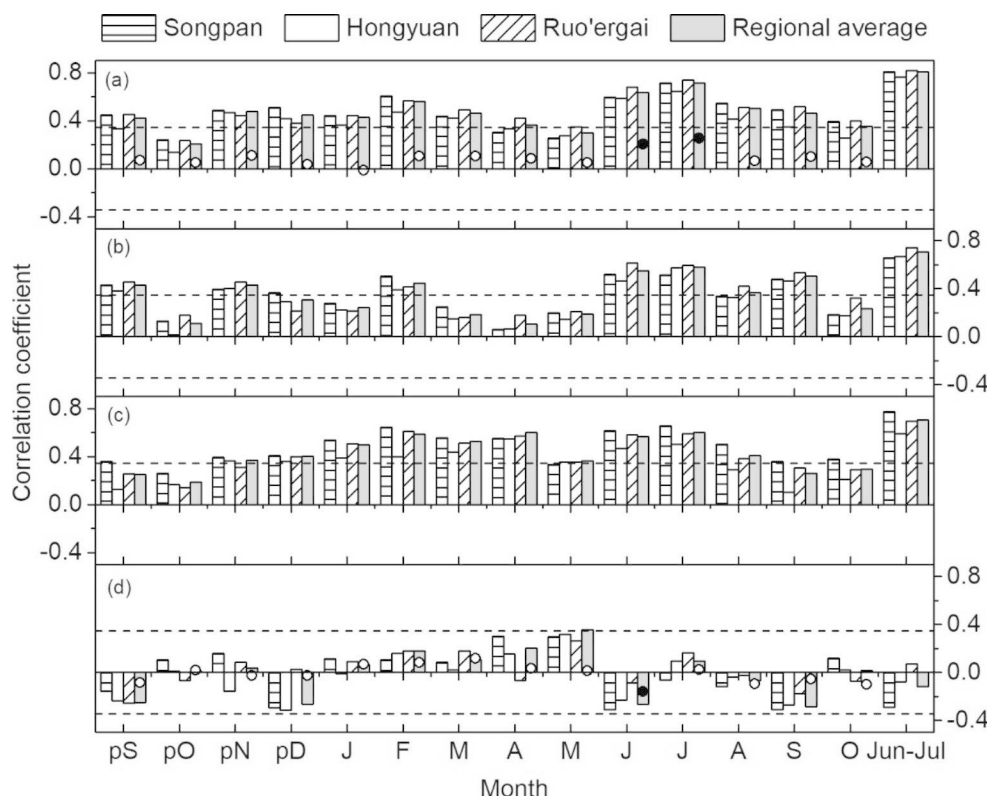
monthly mean temperature (Fig. 4a, b, and c). The two highest correlations occur in June and July. On the other hand, precipitation shows weak correlations with radial growth, with only a marginally significant correlation in current May (Fig. 4d). When seasons are considered, the highest correlation was found between the chronology and June-July mean temperature (r = 0.81, p < 0.001). Furthermore, response functions were calculated between the chronology and regional monthly mean temperature and monthly total precipitation. The results show that June and July temperatures and June precipitation are significant. Since June precipitation is non-significantly correlated with tree growth in terms of correlation analysis, we choose June-July mean temperature as the reconstruction target.

3.3 Reconstruction of June-July mean temperature

We reconstructed June-July mean temperature for the period 1730–2015 using a simple linear regression model (Fig. 5a). The reconstruction accounted for 65.6% of the actual temperature variance during the calibration period 1961–2015. In order to evaluate the reliability of the relationship between tree growth and June-July temperature, we applied the split sample calibration and verification method. As shown in Table 2, the correlation coefficients are all significant at the 99% confidence level, and the reduction of error (RE) and the coefficient efficiency (CE) are all positive, even for the first-order difference series. The final reconstruction is from

1730 to 2015 (Fig. 5b). The mean and standard deviation (SD) of the reconstruction are adjusted to match those of the instrumental data over their common period.

The mean value of the reconstructed June-July temperature series over 1730–2015 is 10.7 °C, and the SD is 0.8 °C. Warm intervals are 1735–1809, 1932–1967 and 1984–2015, while relatively cold conditions prevail in 1810–1931. Extremely warm early summers (> mean + 1.5SD) are 1739, 1776, 1785, 1805, 1997, 1998, 2000, 2001, 2005–2007 and 2009–2015, while extremely cold early summers (< mean − 1.5SD) include 1779, 1837, 1841–1844, 1852, 1864, 1869–1877, 1916 and 1918. A general warming trend can be observed since the 1870s. The most recent warming period starting from the 1980s reached an unprecedented level since the late 1990s. The last two decades (1996–2015) are the warmest in the context of the past 286 years, with 14 out of the 20 years being extremely warm years.

4 Discussion

4.1 Spatial representativeness and characteristics of the reconstructed June-July mean temperature

The reconstructed temperature series can represent the whole eastern Tibetan Plateau and a large part of central western China in terms of both raw and first-differenced data (Fig. 6). The first-differenced series excludes long-term

Fig. 5 a Comparison of the observed (solid line) and reconstructed (dotted line) June-July mean temperature during 1961–2015. **b** Reconstructed June-July mean temperature over the period 1730–2015 (thin line), its 10-year FFT smoothing (thick line), the mean value (solid horizontal line) and ± 1.5 standard deviation (dotted horizontal line) of the reconstructed temperature series
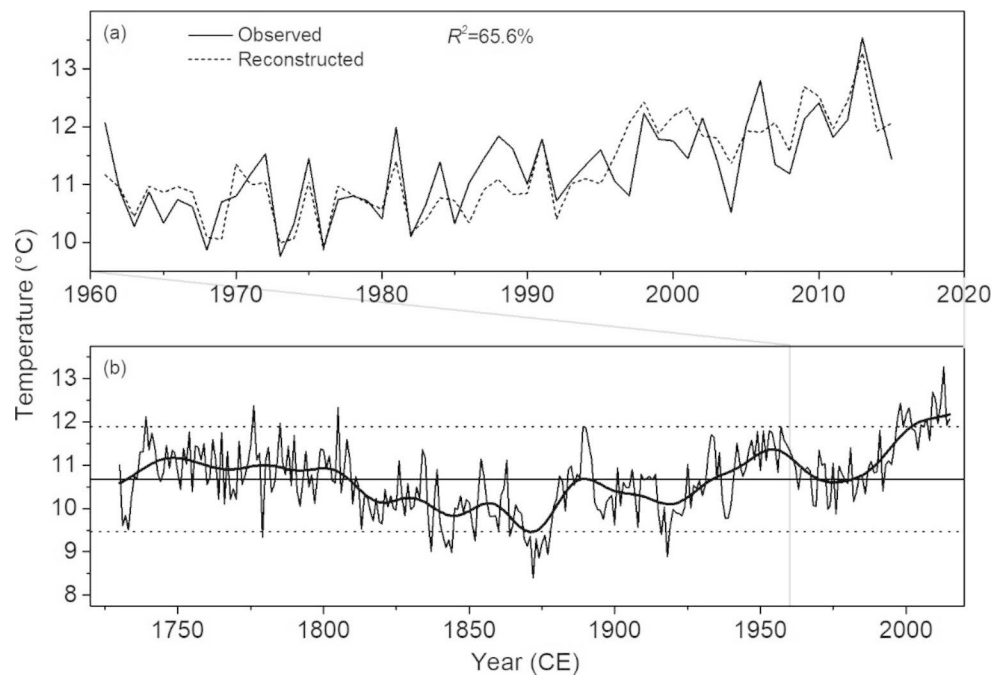
Table 2 Calibration and verification statistics for the common period 1961–2015. The values before and after the slash ("/") denote results for raw and first-differenced data, respectively

Calibration period	r	R^2	Verification period	RE	CE
Full period (1961–2015)	0.810/0.678	0.656/0.459		-	-
Early half (1961–1987)	0.745/0.767	0.556/0.588	Late half (1988–2015)	0.733/0.289	0.201/0.289
Late half (1988–2015)	0.662/0.576	0.438/0.332	Early half (1961–1987)	0.824/0.508	0.396/0.508

Fig. 6 Spatial correlations of instrumental **a**, **b** and reconstructed **c**, **d** June-July mean temperature series with the CRU TS4.03 land temperature over 1961–2015 for raw **a**, **c** and first differenced **b**, **d** data. Non-significant correlations ($p \geq 0.1$) are masked out. The green squares denote the sampling sites of this study. The yellow, blue, white and orange triangles denote the sampling sites of Liang et al. (2008), Yu et al. (2012), Xiao et al. (2015), and Zhu et al. (2016), respectively
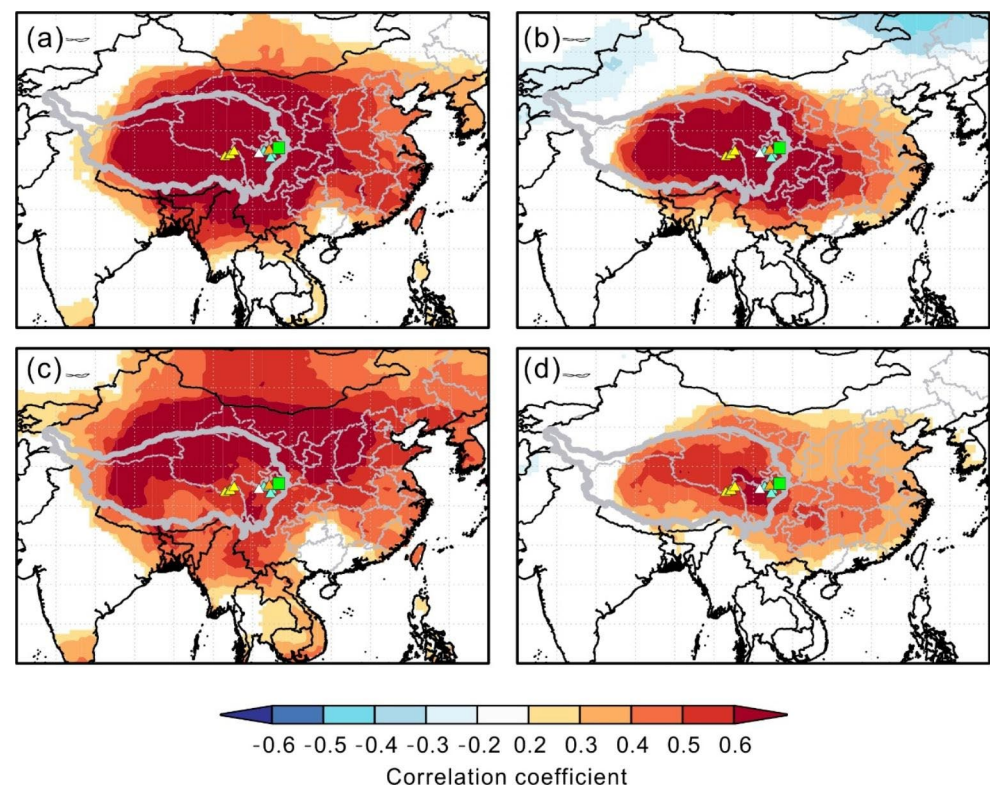
trends and low-frequency signals and represents high-frequency signals. Using the first-differenced series to make a spatial correlation analysis could avoid information inflation which may be caused by low-frequency signals and trends. In terms of the first-difference analysis results, the reconstructed temperature can represent at least the TP to a relatively reliable level (Fig. 6d). Another feature is that there is a distinct temperature difference between the western and eastern China, which is also evidently shown in April-July mean temperature from the southeastern China (Shi et al. 2017a). The topography and temperature differences between the western and eastern China of the same latitude may make atmospheric circulation (i.e., the East Asian monsoon and South Asian monsoon) more complex.

We compared our reconstructed series with other warm-season temperature reconstructions (Fig. 7), including June-August minimum temperature of Liang et al. (2008), June-July minimum temperature of Yu et al. (2012), July-September mean temperature of Xiao et al. (2015), and July-August maximum temperature of Zhu et al. (2016). These reconstructed temperature series have close seasonal windows and similar climate characteristics with ours and represent the best series that could be used for comparison.
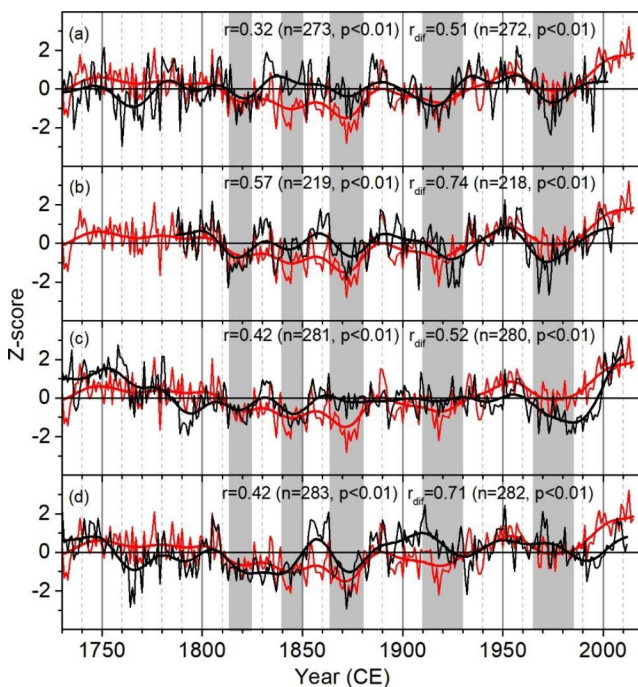

Fig. 7 Comparison of the reconstructed June-July mean temperature (red line) with tree-ring based warm-season temperature reconstructions in the nearby regions (black line). **a** June-August minimum temperature of Liang et al. (2008), b June-July minimum temperature of Yu et al. (2012), c July-September mean temperature of Xiao et al. (2015), and d July-August maximum temperature of Zhu et al. (2016). All series were standardized over their common period 1787–2002, and the bold lines denote the 10-year FFT smoothing. Gray bars denote cold periods in the reconstructions

As shown, they matched well in most periods, such as the relatively cold periods of 1813–1825, 1840–1850 1864–1880, 1910–1930 and 1965–1985, and the warm periods of 1880–1900, 1930–1965, and 1985-present. The reconstruction of this study is significantly correlated with all other reconstructions at 0.01 level, and the correlations between first-differenced series are considerably higher than those between raw series (Fig. 7), indicating that these tree-ring based reconstructions are more consistent on high-frequency variability. Since the reconstructions are based on tree rings from different locations, climatic homogeneity must be responsible for their consistency.

As for the unstable consistency at low frequency, there are several possible reasons, such as ecological disturbance, local microenvironment, different limiting climatic factors on tree growth, and even human disturbance. In order to evaluate whether there are ecological and/or human disturbances on tree growth, one feasible way is to develop two or more independent site chronologies that have the same limiting climatic factors, and then the consistency of these chronologies can be carefully checked to assess the quality of the chronology in reflecting climatic change. Two site chronologies that meet the above criteria were developed in our study (Fig. 2). The correlations between them are very high, 0.84 for the original series and 0.88 for the first differenced series over the period 1748–2015. Furthermore, the series matched very well visually. The high consistency indicates that it is unlikely that ecological or human disturbances affect the quality of the SP0102 chronology used for our June-July temperature reconstruction.

The reconstructed June-July temperature series can be divided into three major periods, i.e., 1730-1800 s, 1810-1930 s, and 1940s-present (Fig. 5b). The first period features warm temperature with major interannual variability. The second period is cold with large decadal variability. The third period features warm temperature with large decadal variability and a recent rapid warming that reached an unprecedented level in the past two decades. Cloud-radiation feedback may plan an important role in modulating the recent warming (Duan and Xiao 2015) which is also likely a response to the increasing greenhouse gases emissions suggested by two coupled global climate models (Duan et al. 2006). The unprecedented warming caused some mixed environmental changes, such as accelerated glacier retreat, early snowmelt, permafrost degradation, increased net primary production, extended agricultural land area, and increased river runoff contributed by mountain glacier melt (Chen et al. 2015; Kang et al. 2010; Yao et al. 2012).
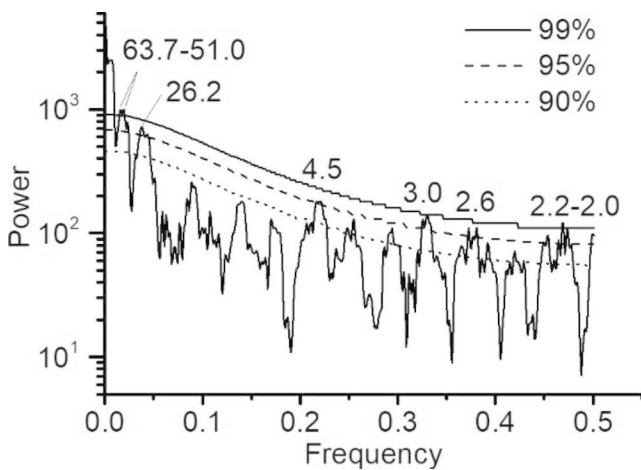
Fig. 8 Results of multi-taper method spectrum analysis of the reconstructed temperature. The solid, dashed and dotted lines indicate the 99%, 95% and 90% confidence levels, respectively

4.2 Periodicity and teleconnections of June-July mean temperature

MTM analysis revealed that the reconstructed temperature series has periodicities of 63.7–51.0, 26.2, 4.5, 3.0, 2.6 and 2.2-2.0 years at 95% confidence level (Fig. 8). The multidecadal scale cycles fall in the typical periodical range of the Atlantic Multidecadal Oscillation (AMO), and the interannual scale cycles correspond to those of El Niño-Southern Oscillation (ENSO). Therefore, the reconstructed temperature series was compared with the AMO and ENSO series to explore their relationship. Mann et al. (2009) employed a diverse multiproxy network comprising more than a thousand tree-ring, ice core, coral, sediment, and other assorted records to reconstruct global patterns of surface temperature changes over the past 1,500 years, with a decadal-resolution. The decadal-scale AMO series was produced by averaging the spatial temperatures of the corresponding region. Wang et al. (2017) used 46 annually resolved terrestrial proxy records including tree-ring, ice core, and document from the circum-North Atlantic-Arctic region to reconstruct the extended summer (May-September) Atlantic Multidecadal Variability index since 800 CE. Li et al. (2013) used 2,222 tree-ring chronologies from both the tropics and mid-latitudes in both hemispheres to reconstruct a seven-century-long ENSO series. The reconstructed temperature series is significantly correlated with both AMO series at 0.01 level, and the correlation coefficients are 0.37 and 0.42 respectively (Fig. 9). However, the correlation between the temperature reconstruction and ENSO series is not significant.

The relationship between the reconstructed temperature and the Pacific Decadal Oscillation (PDO) was also investigated in this study. The PDO is a long-lived El Niño-like pattern of Pacific climate variability. The PDO series is based on observations (Mantua et al. 1997; Zhang et al. 1997), and is defined as the leading principal component of North Pacific sea surface temperature variability. The correlation coefficient is only -0.12, not significant at the 0.05 level (Fig. S2). Therefore, the impact of the PDO on June-July temperature in the eastern TP is very low, which was also found using a spatial correlation analysis by Wang et al. (2014).

AMO has modulated temperature variations of the Tibetan Plateau and its surroundings over the past several centuries, i.e., February-July mean temperature in southwest China (Fang et al. 2019), winter, summer, and annual mean

Fig. 9 Comparison between the temperature reconstruction and two AMO series. The black curves are the reconstructed temperature series. Thin line is original with annual resolution. Thick line is the 10-year FFT smoothing of the original series. **a** The annual-resolution AMO series (thin red line) and its 10-year FFT smoothing (thick red line) from Wang et al. (2017). **b** The decadal-resolution AMO series (thick red line) from Mann et al. (2009)
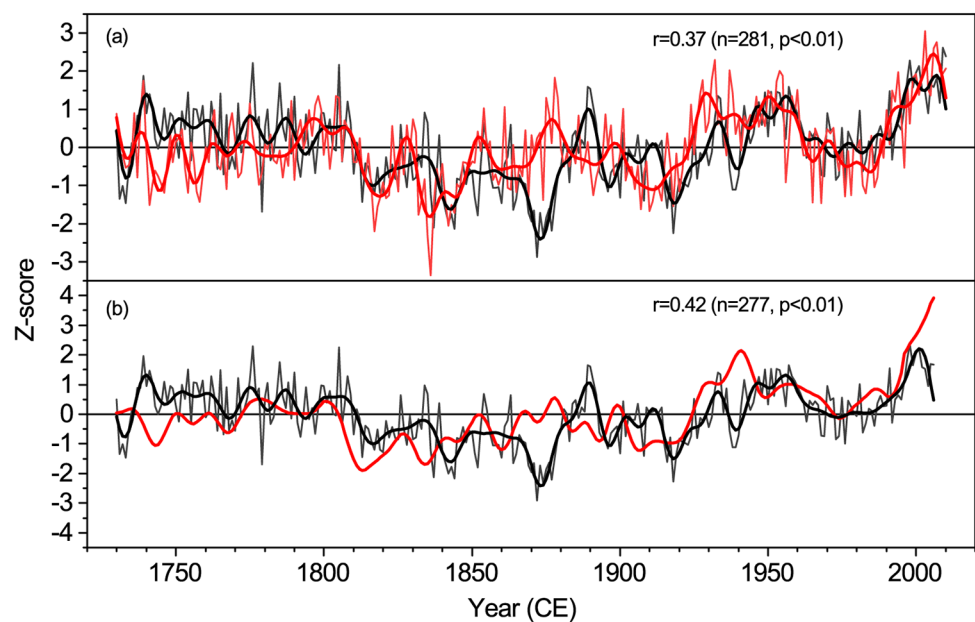
temperatures in the southeastern TP (Shi et al. 2017b; Wang et al. 2014, 2015). AMO is also a factor in modulating early summer temperature on the central eastern TP over the past three centuries. Its influences are realized by warming Eurasian middle and upper troposphere, which may be related to the wave guidance mechanism associated with the Asian upper jet (Wang et al. 2009). Both observations and simulations with an atmospheric circulation model indicate that the AMO warm phase can induce a zonal dipole response in sea level pressure across the Atlantic-Eurasia region, with negative surface air pressure anomalies over the North Atlantic (Knight et al. 2006), and high surface air pressure anomalies and corresponding downward atmospheric motion over the TP, causing negative rainfall and positive temperature anomalies over the TP (Shi et al. 2019). The AMO was in a warm phase over the past two decades, which may have contributed to the unprecedented warming to some extent. The warming was also caused by the increasing greenhouse gases and modulated by cloud-radiation feedback. However, the relative contributions of different driving factors are still uncertain, which is worth of further studies.

5 Conclusion

A robust 286-year chronology was developed from tree-rings collected from two sites on the central eastern Tibetan Plateau. Based on the chronology, June-July mean temperature was reconstructed using a linear regression function that passes all commonly used test parameters, with an explained variance of 65.6%. The recent two decades are the warmest in the past 286 years, with 14 out of 20 years being extremely warm, which clearly shows the unprecedented warming conditions of the last two decades on the central eastern TP. The unprecedented warming will inevitably exert its influence on both mountain glaciers and ecosystems, and further affect the Asian monsoon system, to which enough attention should be paid by the policy-makers. Although the contribution of the AMO to June-July temperature changes was emphasized, the driving forces of temperature changes on the TP are undetermined partly because of its complex topography, spatial heterogeneities and data quality. Therefore, more high-quality and highly replicable temperature reconstructions, like the one in this study, should be produced in different climatic regions of the TP, in order to have an in-depth understanding of the driving forces.

Declarations

References

Bi Y, Cory W, Fan Z, Yang J, Wu Z, Huang W et al (2020) Ring-widths of Abies at tree-line ecotone reveal three centuries of early winter season temperature changes in Yunnan. China Clim Dyn 55(3):945–959. https://doi.org/10.1007/s00382-020-05303-5

Biondi F, Waikul K (2004) DENDROCLIM2002: a C + + program for statistical calibration of climate signals in tree-ring chronologies. Computers Geosci 30(3):303–311. https://doi.org/10.1016/j.cageo.2003.11.004

Bräuning A, Mantwill B (2004) Summer temperature and summer monsoon history on the tibetan plateau during the last 400 years recorded by tree rings. Geophys Res Lett 31(24). https://doi.org/10.1029/2004gl020793

Broccoli AJ, Manabe S (1992) The effects of orography on midlatitude northern hemisphere dry climates. J Clim 5(11):1181–1201. https://doi.org/10.1175/1520-0442(1992)005<1181:Teooom>2.0.Co;2

Chen DL, Xu BQ, Yao TD, Guo ZT, Cui P, Chen FH (2015) Assessment of past, present and future environmental changes on the Tibetan Plateau (in chinese with English abstract). Chin Sci Bull 60(32):3025–3035. https://doi.org/10.1360/N972014-01370

Cook ER (1985) A time series analysis approach to tree-ring standardization. University of Arizona, Tucson, Ph.D.)

Cook ER, Buckley BM, D'Arrigo RD, Peterson MJ (2000) Warm-season temperatures since 1600 BC reconstructed from tasmanian tree rings and their relationship to large-scale sea surface temperature anomalies. Clim Dyn 16(2–3):79–91

Duan A, Xiao Z (2015) Does the climate warming hiatus exist over the tibetan. Plateau? Sci Rep 5(1):13711. https://doi.org/10.1038/srep13711

Duan A, Wu G, Zhang Q, Liu Y (2006) New proofs of the recent climate warming over the Tibetan Plateau as a result of the increasing

greenhouse gases emissions. Chin Sci Bull 51(11):1396–1400. https://doi.org/10.1007/s11434-006-1396-6

Duan JP, Ma ZG, Li L, Zheng ZY (2019) August-September temperature variability on the Tibetan Plateau: past, present, and future. J Geophys Res-Atmos 124(12):6057–6068. https://doi.org/10.1029/2019jd030444

Esper J, Cook ER, Schweingruber FH (2002) Low-frequency signals in long tree-ring chronologies for reconstructing past temperature variability. Sci 295(5563):2250–2253

Fang K, Guo Z, Chen D, Wang L, Dong Z, Zhou F et al (2019) Interdecadal modulation of the Atlantic Multi-decadal Oscillation (AMO) on southwest China's temperature over the past 250 years. Clim Dyn 52(3–4):2055–2065. https://doi.org/10.1007/s00382-018-4244-x

Fritts HC, Blasing TJ, Hayden BP, Kutzbach JE (1970) Multivariate techniques for specifying tree-growth and climate relationships and for reconstructing anomalies in paleoclimate. The University of Arizona Press, Tucson

Fu Y, Ma Y, Zhong L, Yang Y, Guo X, Wang C et al (2020) Land-surface processes and summer-cloud-precipitation characteristics in the Tibetan Plateau and their effects on downstream weather: a review and perspective. Nat Sci Rev 7(3):500–515. https://doi.org/10.1093/nsr/nwz226

Gou X, Chen F, Jacoby G, Cook E, Yang M, Peng H, Zhang Y (2007) Rapid tree growth with respect to the last 400 years in response to climate warming, northeastern tibetan Plateau. Int J Clim 27(11):1497–1503. https://doi.org/10.1002/joc.1480

Gou X, Peng J, Chen F, Yang M, Levia DF, Li J (2008) A dendrochronological analysis of maximum summer half-year temperature variations over the past 700 years on the northeastern tibetan Plateau. Theor Appl Climatol 93(3):195–206. https://doi.org/10.1007/s00704-007-0336-y

Hartmann DL, Klein Tank AMG, Rusticucci M, Alexander LV, Brönnimann S, Charabi Y et al (2013) Observations: atmosphere and surface. In: Stocker TF, Qin D, Plattner G-K, Tignor M, Allen SK, Boschung J, Nauels A, Xia Y, Bex V, Midgley PM (eds) Climate change 2013: the physical science basis. Contribution of Working group I to the fifth assessment report of the Intergovernmental Panel on Climate Change. Cambridge University Press, Cambridge, United Kingdom and New York, NY, USA, pp 159–254

Holmes RL (1983) Computer-assisted quality control in tree-ring dating and measurement. Tree-Ring Bull 43(1):69–78

Huang R, Zhu H, Liang E, Liu B, Shi J, Zhang R et al (2019) A tree ring-based winter temperature reconstruction for the southeastern tibetan Plateau since 1340 CE. Clim Dyn 53(5):3221–3233. https://doi.org/10.1007/s00382-019-04695-3

Hughes MK (2002) Dendrochronology in climatology-the state of the art. Dendrochronologia 20(1–2):95–116

Kang SC, Xu YW, You QL, Flugel WA, Pepin N, Yao TD (2010) Review of climate and cryospheric change in the Tibetan Plateau. Environ Res Lett 5(1):015101. https://doi.org/10.1088/1748-9326/5/1/015101

Knight JR, Folland CK, Scaife AA (2006) Climate impacts of the Atlantic Multidecadal Oscillation. Geophys Res Lett 33(17):L17706. https://doi.org/10.1029/2006gl026242

Li C, Yanai M (1996) The Onset and interannual variability of the asian summer monsoon in relation to land–sea thermal contrast. J Clim 9(2):358–375. https://doi.org/10.1175/1520-0442(1996)009<0358:Toaivo>2.0.Co;2

Li JB, Xie SP, Cook ER, Morales MS, Christie DA, Johnson NC et al (2013) El Nino modulations over the past seven centuries. Nat Clim Change 3(9):822–826. https://doi.org/10.1038/Nclimate1936

Liang E, Shao X, Qin N (2008) Tree-ring based summer temperature reconstruction for the source region of the Yangtze River on the Tibetan Plateau. Glob Planet Change 61(3–4):313–320. https://doi.org/10.1016/j.gloplacha.2007.10.008

Liu XD, Chen BD (2000) Climatic warming in the Tibetan Plateau during recent decades. Int J Clim 20(14):1729–1742. https://doi.org/10.1002/1097-0088(20001130)20:14<1729::aid-joc556>3.0.co;2-y

Liu Y, An ZS, Ma HZ, Cai QF, Liu ZY, Kutzbach JK et al (2006) Precipitation variation in the northeastern tibetan Plateau recorded by the tree rings since 850 AD and its relevance to the Northern Hemisphere temperature. Sci China Ser D-Earth Sci 49(4):408–420. https://doi.org/10.1007/s11430-006-0408-3

Liu Y, An ZS, Linderholm HW, Chen DL, Song HM, Cai QF et al (2009) Annual temperatures during the last 2485 years in the mid-eastern Tibetan Plateau inferred from tree rings. Sci China Ser D-Earth Sci 52(3):348–359. https://doi.org/10.1007/s11430-009-0025-z

Mann ME, Lees JM (1996) Robust estimation of background noise and signal detection in climatic time series. Clim Change 33(3):409–445. https://doi.org/10.1007/bf00142586

Mann ME, Zhang Z, Rutherford S, Bradley RS, Hughes MK, Shindell D et al (2009) Global signatures and dynamical origins of the little ice age and medieval climate anomaly. Sci 326(5957):1256–1260. https://doi.org/10.1126/science.1177303

Mantua NJ, Hare SR, Zhang Y, Wallace JM, Francis RC (1997) A Pacific interdecadal climate oscillation with impacts on salmon production. Bull Am Meteorol Soc 78(6):1069–1079. https://doi.org/10.1175/1520-0477(1997)078<1069:Apicow>2.0.Co;2

Melvin TM, Briffa KR (2008) A "signal-free" approach to dendroclimatic standardisation. Dendrochronologia 26(2):71–86

Shao X, Fan J (1999) Past climate on West Sichuan plateau as reconstructed from ring-widths of dragon spruce (in Chinese, with English abstract). Quaternary Sci 19(1):81–89

Shao X, Xu Y, Yin ZY, Liang E, Zhu H, Wang S (2010) Climatic implications of a 3585-year tree-ring width chronology from the northeastern Qinghai-Tibetan Plateau. Quaternary Sci Rev 29(17–18):2111–2122. https://doi.org/10.1016/j.quascirev.2010.05.005

Shi C, Masson-Delmotte V, Daux V, Li Z, Carré M, Moore J (2015) Unprecedented recent warming rate and temperature variability over the east Tibetan Plateau inferred from Alpine treeline dendrochronology. Clim Dyn 45(5/6):1367–1380. https://doi.org/10.1007/s00382-014-2386-z

Shi J, Li J, Zhang DD, Zheng J, Shi S, Ge Q et al (2017a) Two centuries of April-July temperature change in southeastern China and its influence on grain productivity. Sci Bull 62(1):40–45. https://doi.org/10.1016/j.scib.2016.11.005

Shi S, Li J, Shi J, Zhao Y, Huang G (2017b) Three centuries of winter temperature change on the southeastern tibetan Plateau and its relationship with the Atlantic Multidecadal Oscillation. Clim Dyn 49(4):1305–1319. https://doi.org/10.1007/s00382-016-3381-3

Shi C, Sun C, Wu G, Wu X, Chen D, Masson-Delmotte V et al (2019) Summer temperature over the tibetan Plateau modulated by Atlantic Multidecadal variability. J Clim 32(13):4055–4067. https://doi.org/10.1175/JCLI-D-17-0858.1

Stokes MA, Smiley TL (1996) An introduction to Tree-Ring dating. The University of Arizona Press, Tucson

Wang Y, Li S, Luo D (2009) Seasonal response of asian monsoonal climate to the Atlantic Multidecadal Oscillation. J Geophys Res-Atmos 114(D2):D02112. https://doi.org/10.1029/2008jd010929

Wang J, Yang B, Qin C, Kang S, He M, Wang Z (2014) Tree-ring inferred annual mean temperature variations on the southeastern Tibetan Plateau during the last millennium and their relationships with the Atlantic Multidecadal Oscillation. Clim Dyn 43(3–4):627–640. https://doi.org/10.1007/s00382-013-1802-0

Wang JL, Yang B, Ljungqvist FC (2015) A millennial summer temperature reconstruction for the eastern tibetan Plateau from tree-ring width. J Clim 28(13):5289–5304. https://doi.org/10.1175/Jcli-D-14-00738.1

Wang JL, Yang B, Ljungqvist FC, Luterbacher J, Osborn TJ, Briffa KR, Zorita E (2017) Internal and external forcing of multidecadal Atlantic climate variability over the past 1,200 years. Nat Geosci 10(7):512–517. https://doi.org/10.1038/Ngeo2962

Wei Z, Huang R, Dong W (2003) Interannual and interdecadal variations of air temperature and precipitation over the Tibetan Plateau (in chinese with English abstract). Chin J Atmos Sci 27(2):157–170

Wigley T, Briffa KR, Jones PD (1984) On the average value of correlated time-series, with applications in dendroclimatology and hydrometeorology. J Clim Appl Meteor 23(2):201–213. https://doi.org/10.1175/1520-0450(1984)023<0201:otavoc>2.0.co;2

Wu G, Liu Y, He B, Bao Q, Duan A, Jin F-F (2012) Thermal controls on the asian summer monsoon. Sci Rep 2(1):404. https://doi.org/10.1038/srep00404

Xiao D, Qin N, Li J, Li Y, Mu L (2015) Change of mean temperature from July to September in Northeast of Western Sichuan Plateau based tree-ring (in chinese with English abstract). Plateau Meteor 34(3):762–770

Xu X, Dong L, Zhao Y, Wang Y (2019) Effect of the asian water tower over the Qinghai-Tibet plateau and the characteristics of atmospheric water circulation (in chinese with English abstract). Chin Sci Bull 64(27):2830–2841. https://doi.org/10.1360/TB-2019-0203

Yang B, Qin C, Bräuning A, Osborn TJ, Trouet V, Ljungqvist FC et al (2021) Long-term decrease in asian monsoon rainfall and abrupt climate change events over the past 6,700 years. Proc Natl Acad Sci 118(30):e2102007118. https://doi.org/10.1073/pnas.2102007118

Yao T, Thompson L, Yang W, Yu W, Gao Y, Guo X et al (2012) Different glacier status with atmospheric circulations in Tibetan Plateau and surroundings. Nat Clim Change 2(9):663–667. https://doi.org/10.1038/nclimate1580

Yao TD, Xue YK, Chen DL, Chen FH, Thompson L, Cui P et al (2019) Recent third Pole's rapid warming accompanies cryospheric melt and water cycle intensification and interactions between monsoon and environment: multidisciplinary approach with observations, modeling, and analysis. Bull Amer Meteor Soc 100(3):423–444. https://doi.org/10.1175/Bams-D-17-0057.1

Yu S, Yuan Y, Wei W, Shang H, Zhang T, Chen F, Zhang R (2012) Reconstruction of minimum temperature field in June-July during 1787–2005 in the west Sichuan Plateau (in chinese with English abstract). J Desert Res 32(4):1010–1016

Zhang Y, Wallace JM, Battisti DS (1997) ENSO-like interdecadal variability: 1900-93. J Clim 10(5):1004–1020. https://doi.org/10.1175/1520-0442(1997)010<1004:Eliv>2.0.Co;2

Zhang Q-B, Evans MN, Lyu L (2015) Moisture dipole over the Tibetan Plateau during the past five and a half centuries. Nat Commun 6:8062. https://doi.org/10.1038/ncomms9062

Zhu L, Zhang Y, Li Z, Guo B, Wang X (2016) A 368-year maximum temperature reconstruction based on tree-ring data in the northwestern Sichuan Plateau (NWSP), China. Clim Past 12(7):1485–1498. https://doi.org/10.5194/cp-12-1485-2016